Advanced Materials Science

Research Article ISSN: 2398-6883

Preparation of various morphologies of ZnO nanostructure through wet chemical methods

Nguyen Dac Dien*

Vietnam Trade Union University, Dong Da, Hanoi, Vietnam

Abstract

Hydrothermal route and solution reaction method are adopted for the synthesis of zinc oxide (ZnO) nanopowders having four different morphologies such as nanoparticle, mirorod, nanoplate and nanotubule. Zinc nitrate hexahydrate $Zn(NO_3)_2.6H_2O$ was used as precursor for ZnO nanostructures. ZnO nanorods and nanoplates were synthesized by a hydrothermal approach using KOH as reaction chemical. ZnO nanotubes were obtained by a chemical reaction of $Zn(NO_3)_2$ and NH_4OH. And ZnO nanoparticles were prepared by precipitation method from zinc nitrate and ammonium carbonate $(NH_4)_2CO_3$ in aqueous solution. The structures, morphology, and element components of these ZnO products fabricated by the above-mentioned methods were characterized by X-ray diffraction (XRD), scanning electron microscopy (SEM) and transmission electron microscopy (TEM). These experimental results demonstrated that the as-prepared ZnO nanoparticles have average diameter of 30-60 nm; rod-like ZnO has average diameter of about 350 nm and the length of 3.5 μm; plate-like ZnO has average thickness of about 40 nm and lateral size of 200 × 400 nm; ZnO nanotubules have outer diameter of about 400 nm and inner diameter of about 300 nm, the length of about 4 μm. The XRD results indicated that four morphologies of ZnO are all wurtzite structure. It is found that the wet chemical technique is very promising for fabricating ZnO nanocrystallines with various morphologies.

Introduction

ZnO nanostructures have attracted much attention in recent years due to unique optical, electrical properties compared with their bulk counterparts as well as their size-dependent optical and electrical characteristics, which have encouraged many researchers to investigate ZnO nanomaterials. The properties of the ZnO nanomaterials strongly depended on the microstructures of the materials such as crystal size, morphology (how the crystals are stacked), orientation, aspect ratio, crystalline density [1]. Nano-sized zinc oxide is frequently studied because of its interest in fundamental science as well its applied aspects in many areas, including chemical sensor [2-7], biosensors [8], photocatalysis [9,10], solar cell [11], electrochemical cells [12], ultraviolet lasers [13-15], light-emitting diodes [16], flat panel displays [17], etc. Hitherto, synthesizing uniform nanosized ZnO material is of great important due to its various attractive properties and potential applications. So various methods have been adopted for the fabrication of ZnO nanostructures such as direct precipitation [18-21], sol-gel [19], hydrothermal method [22,23], wet chemical method [8,24,25], thermal evaporation [7,26], etc. Among these techniques, low-temperature wet chemical processes such as precipitation and hydrothermal methods are cost-effective and excellent routes for synthesizing various nanomaterials. The precipitation process has been successfully used to design different structures of ZnO [27]. The hydrothermal process is relatively easy to perform and allows us to tailor the morphology of the products by controlling the components of the solution reaction and hydrothermal conditions. Hydrothermal method also provides a low cost and large-scale production. It does not need expensive raw materials and complicated equipment. This method shows the reliability, repeatability and simplicity compared with other methods.

In recent years, scientists have made some advancement in fabricating metal oxide nanostructures using hydrothermal route. For example, Yani Li et al. prepared tungsten oxide nanorods by microwave hydrothermal method [28], Choong-Yong Lee synthesized WO_3 hollow microspheres by one-pot hydrothermal reaction of an aqueous solution containing glucose and sodium tungstate [29], Xuchun Song et al. fabricated tungsten oxide nanobelts by hydrothermal technique using CTAB as assisting agent [30], Jun Zhang et al. synthesized α-Fe_2O_3@ZnO core-shell nanospindles via a two-step hydrothermal approach [31], O. Lupan and his colleagues obtained SnO_2 nanorods via a hydrothermal treatment [32], ZnO nanorods and nanoparticles have been synthesized by hydrothermal technique [33], iron oxide was prepared through microwave hydrothermal route using ferrous sulphate and sodium hydroxide as starting chemicals [34]. Various metal oxides were also synthesized by hydrothermal methods such as Sn_3O_4 [35], $FeWO_4$ [36], TiO_2 [37,38], ZrO_2 [39], etc. As the morphology and structure of a material depend upon synthesis conditions and parameters, therefore, various precursors and additives are used in aqueous medium to successfully synthesize ZnO nanostructures bearing different geometries. It is suggested that the growth mechanism of the ZnO nanostructures is self-aggregation and oriented aggregation. In the present study, the nano-sized ZnO structures were synthesized by a direct precipitation method and a hydrothermal method. These methods in comparison with the other methods have their own advantages such as low-processing cost, high quality and high manufacture yield. A detailed comparison of

Correspondence to: Nguyen Dac Dien, Vietnam Trade Union University, 169 Tay Son, Quang Trung, Dong Da, Hanoi, Vietnam, Tel: 0975528087; E-mail: diennd@dhcd.edu.vn

Key words: *ZnO nanostructure, precipitation method, hydrothermal treatment, wet chemical technique, characterization*

Received: December 28, 2018; **Accepted:** January 18, 2019; **Published:** January 21, 2019

the crystalline size, morphology, structure and composition of ZnO products synthesized by the above mentioned methods was made.

Experimental

Synthesis of ZnO nanoparticles

All chemical reagents used in this experiment were of analytical grade. The detailed synthesis procedure was described as follows. Zinc nitrate hexahydrate $Zn(NO_3)_2.6H_2O$ (3.7125 g) was added to 200 ml of distilled water (high-purity water) to obtain the solution concentration of $Zn(NO_3)_2$ of 0.0625 M. Then, 2.25 g ammonium carbonate trihydrate $(NH_4)_2CO_3.3H_2O$ was dissolved in 240 ml of distilled water to become 0.0625 M $(NH_4)_2CO_3$ solution. Subsequently, $(NH_4)_2CO_3$ solution was slowly dropped into the vigorously stirred $Zn(NO_3)_2$ solution with molar ratio of 1:1.2 for 1 h. The reaction between $Zn(NO_3)_2$ and $(NH_4)_2CO_3$ solutions yields the white precipitate:

$$Zn(NO_3)_2+(NH_4)_2CO_3 \rightarrow ZnCO_3\downarrow+2NH_4NO_3 \quad (1)$$

The white precipitate ($ZnCO_3$) was collected by filtration and repeated washed with water and absolute ethanol several times then dried at 80°C overnight. The final product of porous particle-like ZnO nanostructure was obtained by annealing the as-prepared precursor at 500°C for 2 h in a tube furnace. $ZnCO_3$ turns into ZnO following the thermal decomposition of the precursor:

$$ZnCO_3 \rightarrow ZnO+CO_2\uparrow \quad (2)$$

Synthesis of ZnO nanoplates

ZnO nanoplates were synthesized using method reported previously [40]. In a typical experiment, 7.512 g $Zn(NO_3)_2.6H_2O$ was dissolved into 50 ml of deionized water. Then, 83 ml 1.5 M KOH solution was added drop wise under constant magnetic stirring for 15 minutes. After that, the resulting mixture solution was sealed in a Teflon-lined stainless-steel autoclave of 200 ml capacity. The autoclave was heated to 180C and maintained for 20 h. After cooling down to room temperature naturally, the white precipitate was harvested and rinsed with distilled water and absolute ethanol several times and finally dried in air at 80°C overnight for further characterization. The reactions happened in the producing process containing:

$$Zn(NO_3)_2+2KOH \rightarrow Zn(OH)_2\downarrow+2KNO_3 \quad (3)$$

$$Zn(OH)_2 \rightarrow ZnO+H_2O \quad (4)$$

Synthesis of ZnO microrods

The procedure for producing ZnO microrods using the hydrothermal route is similar to that of ZnO nanoplates presented above. The only difference between two techniques is the hydrothermal time (48 h instead of 20 h).

Synthesis of ZnO nanotubules

Zinc nitrate hexahydrate $Zn(NO_3)_2.6H_2O$, ammonia solution NH_4OH (25%), absolute ethanol (C_2H_5OH, purity 99.7%) and deionized water were used in the experiment. The detailed synthesis procedure was described as follows. Firstly, 0.925 g $Zn(NO_3)_2.6H_2O$ was dissolved in 100 ml distilled water at room temperature and stirred for 30 minutes to obtain the transparent solution. Then, 9.5 ml NH_4OH solution was slowly dropped into the $Zn(NO_3)_2$ solution. The mixture solution was stirred constantly using the magnetic stirrer for 2 h. Precipitation was made in this process as following:

$$Zn(NO_3)_2+6NH_4OH \rightarrow Zn(NH_3)_4(OH)_2++2NH_4NO_3+4H_2O \quad (5)$$

$$Zn(NH_3)_4(OH)_2 \rightarrow ZnO+4NH_3+H_2O \quad (6)$$

In order to remove the by-products and remnants bound to the nanotubules, the precipitate was washed with ethanol and distilled water repeatedly. At last, the precursors were dried in the muffle furnace at 80°C overnight. Zinc hydroxide was dehydrated to form ZnO which is described by equation (4). The white powder of the ZnO nanotubules was obtained after heating at 600°C for 2 h.

Results and discussion

SEM analysis

Figure 1 shows the scanning electron micrographs (SEM) and the transmission electron micrograph (TEM) of ZnO nanoparticles prepared by direct precipitation method. This figure reveals that the ZnO nanoparticles have particle-like morphology with the diameter in the range of 30-60 nm.

Figure 2a shows the scanning electron microscopy (SEM) photograph of the ZnO nanoplates. Transmission electron microscopy (TEM) was also used to observe the surface state of ZnO nanoplates in order to further determine the morphology of the ZnO, and the result shown in Figure 2b indicated that the plates are about 40-50 nm in thickness with neat shape. Figure 2c shows ZnO nanoplates with the lateral size of 200 × 400 nm in higher resolution. There was no considerable difference in the plate dimension. Furthermore, smooth surface confirmed few crystal defects on the surface of the ZnO plates.

Figure 3 obviously shows that the as-prepared ZnO powder sample synthesized through hydrothermal route at 180°C for 48 h consists of relatively uniform and smooth surface rod-like micro-structures with length of 3.5 μm and hexagonal cross section with diameter of 350 nm. The possible formation mechanism for rod-like and plate-like ZnO structures was given in Figure 4.

The precursor precipitates of zinc oxide (ZnO) were obtained via the reaction between zinc nitrate $Zn(NO_3)_2$ and potassium hydroxide KOH in aqueous solution. The precursor of ZnO is benificial to the formation of nanoplate structure in the hydrothermal process. When the hydrothermal time was prolonged, the nanoplates present preferential-oriented aggregation and growth at [002] direction and ZnO microrods with the aspect ratio of 10 are synthesized. The formation of rod-like and plate-like ZnO is closely related to each other. It was found that the precursor of reactants, hydrothermal temperature and time were the key factors for preparing ZnO materials.

Figure 5 shows the SEM micrograph of tubular ZnO synthesized by precipitation method from $Zn(NO_3)_2$ and NH_4OH. It can be seen from Figure 5a that the tubular ZnO is composed of a number of non-uniform tubule-like structures which coexist with small irregular nanorods. ZnO product is in tube-shape with an average length of 4 μm, the outer and inner diameters of the hollow tubule with a closed end and an opened end are about 400 nm and 300 nm, respectively. The wall of the tubule of ~100 nm thickness is not smooth due to its build-up by polycrystalline nanoparticles. The magnified hollow structure in the 3D nanostructures could be clearly observed in Figure 5b. The pore structure and the high porosity in ZnO tubules are visible from SEM images. It is found that the products well remain the tube shape without significant destruction after calcination at 600°C for 2 h. The formation of tube-like ZnO may be ascribed to the crystal habit. ZnO is a polar crystal showing positive and negative polar planes, rich in Zn and O [10]. The ZnO nanoparticles formed in the reaction assemble along certain orientations and aggregate into hollow structure. In

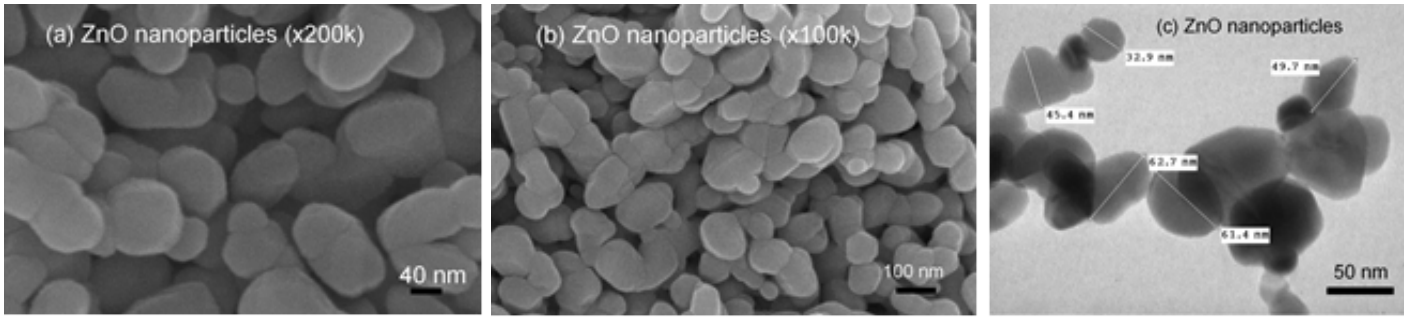

Figure 1. SEM micrographs of ZnO nanoparticles at different magnifications of (a) 200k, (b) 100k, (c) TEM image of ZnO nanoparticles

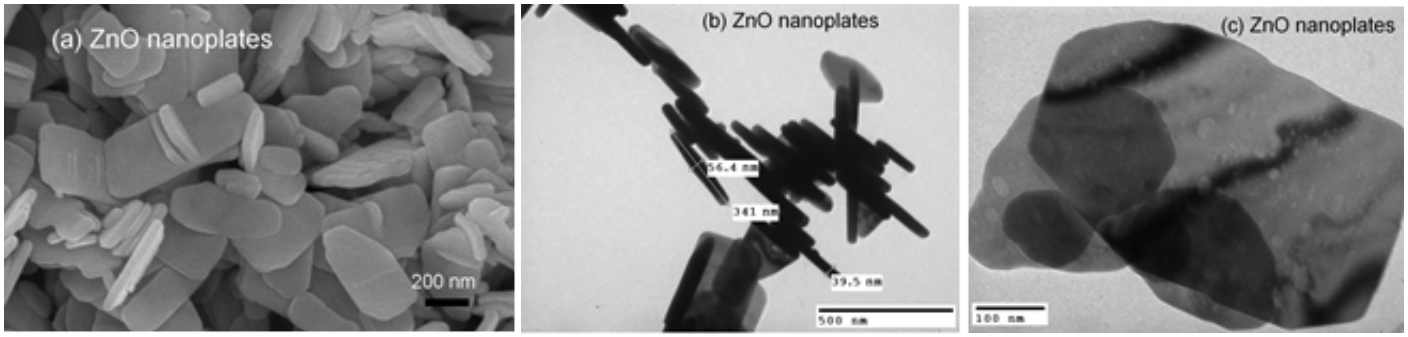

Figure 2. (a) SEM image of ZnO nanoplates at the magnification of 50k, TEM images of ZnO nanoplates at different magnifications of (b) 31.2k and (c) 80.4k

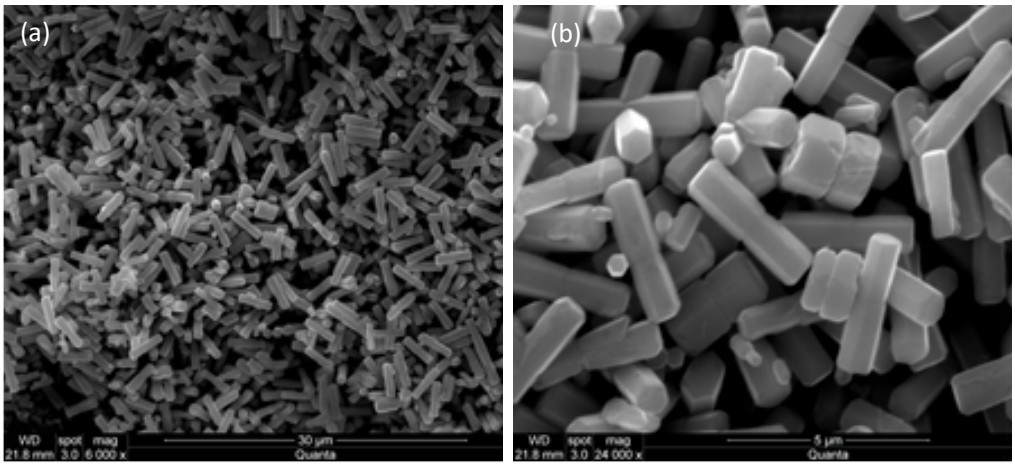

Figure 3. SEM images of ZnO microrods at the magnification of (a) 6k and (b) 24k

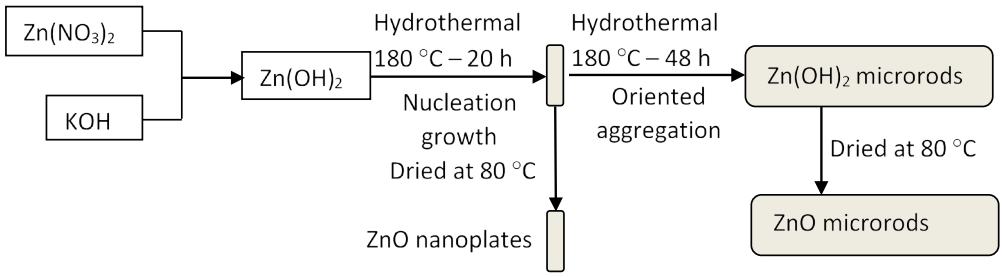

Figure 4. Illustration of the possible formation mechanism for rod-like and plate-like ZnO structures.

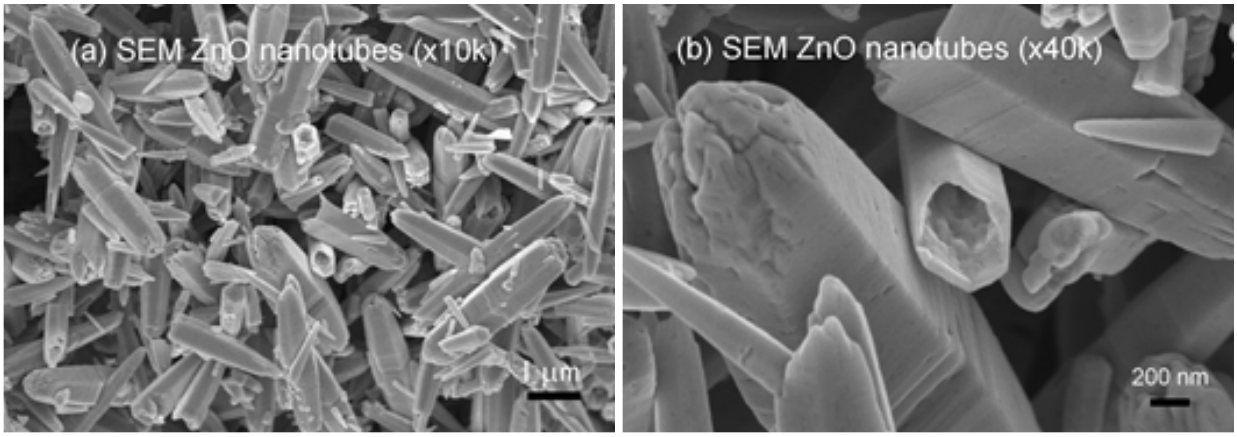

Figure 5. SEM images of tubular ZnO at the magnification of (a) 10k and (b) 40k

2002, Jun Zhang and co-workers (China) [41] synthesized tubular ZnO from $Zn(NH_3)_4^{2+}$ precursor decomposition at 180°C in ethanol. Their tubules had the hollow structures with ~450 nm in diameter and ~4 μm in length. According to Jun Zhang, the solvent ethanol and the temperature are important factors for the formation of tubular ZnO. In this study, though we do not use ethanol as solvent as well as hydrothermal treatment, we obtained obvious hollow structure of ZnO.

XRD analysis

Figure 6 depicts the XRD pattern of the ZnO nanomaterials, which is called the zincite. All of three morphologies have the same hexagonal wurtzite type structure with lattice parameters in accordance with values in the standard card (JCPDS card number 79-0205 for ZnO), where a=b=0.3242 nm, c=0.5188 nm, α=β=90°, γ=120°, space group P6/3mc. Nine peaks appear at 2θ = 31.7°, 34.4°, 36.3°, 47.5°, 56.6°, 62.3°, 66.5°, 67.9°, and 69.1°, which correspond to (100), (002), (101), (102), (110), (103), (200), (112) and (201) planes, respectively. The strong and narrow diffraction peaks in the pattern imply the ZnO nanomaterials with high degree of crystallinity. No characteristic peaks from other impurities were detected in the XRD pattern, confirming the high purity of the synthesized products. As estimated from the half-peak width by Debye-Scherrer's equation:

$$D = \frac{k\lambda}{\beta \cos\theta} \quad (7)$$

where D is the crystalline size, k=0.893 is the Debye-Scherrer constant, λ=0.154056 nm is the X-ray wavelength used in XRD analysis, β is the line broadening at half the maximum intensity (FWHM) in radians and θ is the Bragg diffraction angle [42], the average crystalline size of ZnO nanoplates and nanorods was about 42 nm, and that of ZnO nanoparticles was about 30 nm. The particle size of ZnO nanoparticles (30-60 nm) observed in TEM measurement is more than the crystallite size (30 nm) using XRD measurement, indicating the agglomeration of crystallites in ZnO nanoparticles. Such agglomeration of ZnO nanoparticles was also reported by Davood Raoufi [18], who prepared ZnO nanoparticles with crystalline size in the range of 8.34-27.59 nm by a precipitation method from zinc nitrate and ammonium carbonate. The preferential crystalline orientation was obtained by the Texture coefficient TC(hkl), which has already been reported previously [20] and indicated that the (002) plane was the main preferred growth orientation of the ZnO microrods and tubules.

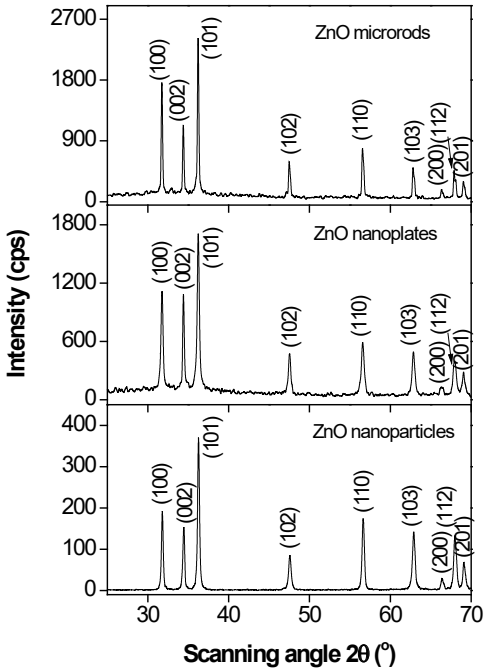

Figure 6. XRD pattern of ZnO microrods, nanoplates and nanoparticles synthesized by hydrothermal treatment

Conclusion

In summary, ZnO nanomaterials with different morphologies have been obtained by the hydrothermal technique and the chemical solution method. The obtained ZnO nanostructures were verified by different methods including SEM, TEM, XRD and EDS measurements. ZnO nanoparticles and nanotubules can be prepared by a wet chemical method and ZnO nanoplates and microrods can be synthesized by a hydrothermal route. Where, ZnO nanoparticles were synthesized by a direct precipitation via $Zn(NO_3)_2/(NH_4)_2CO_3$ as starting materials; ZnO nanotubules from $Zn(NO_3)_2/NH_4OH$ as precursors; ZnO nanoplates and microrods were synthesized by hydrothermal method via $Zn(NO_3)_2$/KOH as starting materials. All the XRD patterns indicated that there was no obvious difference in crystal structure, but the morphology and crystalline size were different. The ZnO nanomaterials formed in this research have promising applications in the development of studying target gases/metal oxide surface interaction and nanosized gas sensors.

Acknowledgments

This research was carried out at School of Engineering Physics, Hanoi University of Science and Technology.

References

1. Liu B, Zeng HC (2003) Hydrothermal synthesis of ZnO nanorods in the diameter regime of 50 nm. *J Am Chem Soc* 125: 4430-4431. [Crossref]
2. Tang H, Yan M, Zhang H, Li S, Ma X, et al. (2006) A selective NH_3 gas sensor based on Fe_2O_3–ZnO nanocomposites at room temperature. *Sens Actuators B Chem* 114: 910-915.
3. Liu Y, Yu J, Lai PT (2004) Investigation of WO3/ZnO thin-film heterojunction-based Schottky diodes for H2 gas sensing. *Int J Hydrogen Energy* 39:10313-10319.
4. Kim SJ, Na CW, Hwang IS, Lee JH (2012) One-pot hydrothermal synthesis of CuO-ZnO composite hollow spheres for selective H2S detection. *Sens Actuators B Chem* 168: 83-89.
5. Huang L, Fan H (2012) Room-temperature solid state synthesis of ZnO/a-Fe_2O_3 hierarchical nanostructures and their enhanced gas-sensing properties. *Sens Actuators B Chem* 171-172: 1257-1263.
6. Huang J, Dai Y, Gu C, Sun Y, Liu J (2013) Preparation of porous flower-like CuO/ZnO nanostructures and analysis of their gas-sensing property. *J Alloys Compd* 575: 115-122.
7. Na CW, Woo HS, Kim ID, Lee JH (2011) Selective detection of NO_2 and C_2H_5OH using a Co3O4-decorated ZnO nanowire network sensor. *Chem Commun (Camb)* 47: 5148-5150. [Crossref]
8. Xia C, Wang N, Lidong L, Lin G (2008) Synthesis and characterization of waxberry-like microstructures ZnO for biosensors. *Sens Actuators B Chem* 129: 268-273.
9. Xie J, Zhou Z, Lian Y, Hao Y, Liu X, et al. (2014) Simple preparation of WO3-ZnO composites with UV-Vis photocatalytic activity and energy storage ability. *Ceram Int* 40: 12519-12524.
10. Lam SM, Sin JC, Abdullah AZ, Mohamed AR (2013) ZnO nanorods surface-decorated by WO3 nanoparticles for photocatalytic degradation of endocrine disruptors under a compact fluorescent lamp. *Ceram Int* 39: 2343-2352.
11. Lee D, Bae WK, Park I, Yoon DY, Lee S, et al. (2011) Transparent electrode with ZnO nanoparticles in tandem organic solar cells. *Sol Energy Mater Sol Cells* vol. 95: 365-368.
12. Weller H (1993) Quantized Semiconductor Particles: A novel state of matter for materials science. *Adv Mater* 5: 88-95.
13. Xu S, Wang ZL (2011) One-dimensional ZnO nanostructures: Solution growth and functional properties. *Nano Res* 4: 1013-1098.
14. Huang MH, Mao S, Feick H, Yan H, Wu Y, et al. (2001) Room-temperature ultraviolet nanowire nanolasers. *Science* 80: 1897-1899.
15. Govender K, Boyle DS, O'Brien P, Binks D, West D, et al. (2002) Room-temperature lasing observed from ZnO nanocolumns grown by aqueous solution deposition. *Adv Mater* 14: 1221-1224.
16. Park WI, Yi GC (2004) Electroluminescence in n-ZnO Nanorod Arrays Vertically Grown on p-GaN. *Adv Mater* 16: 87-90.
17. Mao DS, Wang X, Li W, Liu XH, Li Q, et al. (2002) Electron field emission from hydrogen-free amorphous carbon-coated ZnO tip array. *J Vac Sci Technol B Microelectron Nanom Struct* 20: 278.
18. Raoufi D (2013) Synthesis and microstructural properties of ZnO nanoparticles prepared by precipitation method. *Renew Energy* 50: 932-937.
19. Chen C, Yu B, Liu P, Liu J, Wang L (2011) Investigation of nano-sized ZnO particles fabricated by various synthesis routes. *J Ceram Process Res* 12: 420-425.
20. Wang H, Li C, Zhao H, Liu J (2013) Preparation of nano-sized flower-like ZnO bunches by a direct precipitation method. *Adv Powder Technol* 24: 599-604.
21. Lanje AS, Sharma SJ, Ningthoujam RS, Ahn JS, Pode RB (2013) Low temperature dielectric studies of zinc oxide (ZnO) nanoparticles prepared by precipitation method. *Advanced Powder Technology* 24: 331-335.
22. Gu C, Huang J, Wu Y, Zhai M, Sun Y, et al. (2011) Preparation of porous flower-like ZnO nanostructures and their gas-sensing property. *J Alloys Compd* 509: 4499-4504.
23. Sivapunniyam A, Wiromrat N, Myint MT, Dutta J (2011) High-performance liquefied petroleum gas sensing based on nanostructures of zinc oxide and zinc stannate. *Sens Actuators B Chem* 157: 232-239.
24. Pacholski C, Kornowski A, Weller H (2002) Self-assembly of ZnO: from nanodots to nanorods. *Angew Chem Int Ed Engl* 41: 1188-1191. [Crossref]
25. Rao GT, Rao DT (1999) Gas sensitivity of ZnO based thick film sensor to NH_3 at room temperature. *Sens Actuators B Chem* 55: 166-169.
26. Van Hieu N, Chien ND (2008) Low-temperature growth and ethanol-sensing characteristics of quasi-one-dimensional ZnO nanostructures. *Physica B Condensed Matter* 403: 50-56.
27. Sepulveda-Guzman S, Reeja-Jayan B, de La Rosa E, Torres-Castro A, Gonzalez-Gonzalez V, et al. (2009) Synthesis of assembled ZnO structures by precipitation method in aqueous media. *Mater Chem Phys* 115: 172-178.
28. Li Y, Su X, Jian J, Wang J (2010) Ethanol sensing properties of tungsten oxide nanorods prepared by microwave hydrothermal method. *Ceram Int* 36: 1917-1920.
29. Lee CY, Kim SJ, Hwang IS, Lee JH (2009) Glucose-mediated hydrothermal synthesis and gas sensing characteristics of WO3 hollow microspheres. *Sens Actuators B Chem* 142: 236-242.
30. Song X, Zhao Y, Zheng Y (2006) Hydrothermal synthesis of tungsten oxide nanobelts. *Mater Lett* 60: 3405-3408.
31. Zhang J, Liu X, Wang L, Yang T, Guo X, et al. (2011) Synthesis and gas sensing properties of a-Fe_2O_3@ZnO core-shell nanospindles. *Nanotechnology* 22: 185501. [Crossref]
32. Lupan O, Chow L, Chai G, Heinrich H, Park S, et al. (2009) Synthesis of one-dimensional SnO_2 nanorods via a hydrothermal technique. *Phys E Low-Dimensional Syst Nanostructures* 41: 533-536.
33. Singh O, Singh MP, Kohli N, Singh RC (2012) Effect of pH on the morphology and gas sensing properties of ZnO nanostructures. *Sens Actuators B Chem* 166-167: 438-443.
34. Dhage SR, Khollam YB, Potdar HS, Deshpande SB, Bakare PP, et al. (2002) Effect of variation of molar ratio (pH) on the crystallization of iron oxide phases in microwave hydrothermal synthesis. *Materials Letters* 57: 457-462.
35. Li M, Tan R, Li R, Song W, Xu W (2014) Effects of pH on the microstructures and optical properties of Sn_3O_4 crystals prepared by hydrothermal method. *Ceram Int* 40: 11381-11385.
36. Yu F, Cao L, Huang J, Wu J (2013) Effects of pH on the microstructures and optical property of FeWO4 nanocrystallites prepared via hydrothermal method. *Ceram Int* 39: 4133-4138.
37. Yu J, Su Y, Cheng B, Zhou M (2006) Effects of pH on the microstructures and photocatalytic activity of mesoporous nanocrystalline titania powders prepared via hydrothermal method. *J Mol Catal A Chem* 258: 104-112.
38. Shi X, Tsuru K, Xu L, Kawachi G, Ishikawa K (2013) Effects of solution pH on the structure and biocompatibility of Mg-containing TiO_2 layer fabricated on titanium by hydrothermal treatment. *Appl Surf Sci* 270: 445-451.
39. Hu-Min C, Li-Jun W, Ji-Ming M, Zhi-Ying Z, Li-Min Q (1999) The Effects of pH and Alkaline Earth Ions on the Formation of Nanosized Zirconia Phases Under Hydrothermal Conditions. *J Eur Ceram Soc* 19: 1675-1681.
40. Nguyen DD, Do DT, Vu XH, Dang DV, Nguyen DC (2016) ZnO nanoplates surfaced-decorated by WO3 nanorods for NH_3 gas sensing application. *Adv Nat Sci Nanosci Nanotechnol* 7: 15004.
41. Zhang J, Sun L, Liao C, Yan C (2002) A simple route towards tubular ZnO. *Chem Commun (Camb)*: 262-263. [crossref]
42. Mirabbos H, Raghunath K, Olim R, Yinglin Y, Gangqiang Z, et al. (2012) Besom-like CdWO4 structures composed of single-crystalline nanorods grown under a simple hydrothermal process in ultra-wide pH range. *Opt Mater (Amst)* 34: 1954-1957.